Chapter 1

Fast-spinning and highly magnetized white dwarfs

Edson Otoniel*, Jaziel G. Coelho** ***, Manuel Malheiro†,
and Fridolin Weber ‡ ◇

*Instituto de Formação de Educadores, Universidade Federal do Cariri
Brejo Santo, CE, Brazil
**Departamento de Física, Universidade Tecnológica Federal do Paraná
Medianeira, PR, Brazil
***Divisão de Astrofísica
Instituto Nacional de Pesquisas Espaciais
São José dos Campos, SP, Brazil
†Departamento de Física, Instituto Tecnológico de Aeronáutica
São José dos Campos, SP, Brazil
‡Department of Physics, San Diego State University
San Diego, California, USA
◇Center for Astrophysics and Space Sciences
University of California at San Diego
La Jolla, California, USA
*edson.otoniel@ufca.edu.br, **jazielcoelho@utfpr.edu.br, †malheiro@ita.br,
‡fweber@ucsd.edu

As is well known, the existence of fast and ultra-massive white dwarfs has been discovered in recent years. We estimate the mass density thresholds for the onset of electron capture reactions and pycnonuclear reactions in the cores of fast, massive and highly magnetized white dwarfs (HMWDs) and discuss the impact of microscopic stability and rapid rotation on the structure and stability of different WD constitutions. We confirm that fast rotation increases the mass of a WD by up to 10%, while the central density may drop by one to two orders of magnitude, depending on stellar mass and rate of rotation. We also note that the central densities of the rotating WDs are smaller than those of the non-rotating stars, since less pressure is to be provided by the equation of state (EoS) in the rotating case, and that the maximum-mass limit slightly decreases when lattice contributions are taken into account, which soften the EoS mildly. The softening leads to WDs with somewhat smaller radii and

2 *E. Otoniel, J.G. Coelho, M. Malheiro, and F. Weber*

therefore smaller Kepler periods. Overall, one sees that very massive and magnetic $^{12}C +^{16} O$ WDs have rotational Kepler periods on the order of 0.5 s. Pycnonuclear reactions are triggered in these WDs at masses that are markedly smaller than the maximum WD masses. The corresponding rotational periods turn out to be in the 5 second (~ 0.2 Hz) range.

keywords: white dwarfs; rotation; magnetic fields.

Contents

1. Introduction

The increasing data from observational white dwarf (WD) surveys has confirmed the existence of highly magnetized white dwarfs (HMWDs) with surface magnetic fields between 10^6 an 10^9 G (see Kepler et al., 2010, 2013, 2015; Külebi et al., 2009; Külebi et al., 2010, for recent results of the Sloan Digital Sky Survey (SDSS) for HMWDs). Indeed, polar magnetic fields vary from 7 MG (V2301Oph) up to 240 MG (AR UMa) whereas intermediate polar fields have magnitudes of $\sim$ 4-30 MG, with the highest value of $\sim$ 32 MG for V405Aur (Ferrario et al., 2015). For isolated WDs, the magnetic field is in the range of $\sim 10^3 - 10^9$ G. Close to 10^7 G, there are several examples of isolated WDs such as WD 0806+376 with a field of 3.97×10^7 G and WD 1017-367 with $B = 6.5 \times 10^7$ G (see Ferrario et al., 2015, for another examples of HMWDs). Most of them have been shown to be massive

and responsible for the high-mass peak at 1 $M_\odot$ of the white dwarf mass distribution. Examples are the white dwarf REJ 0317–853 which has a mass of $M \approx 1.35$ $M_\odot$ and a magnetic field of $B \approx (1.7\text{–}6.6) \times 10^8$ G (Barstow et al., 1995; Külebi et al., 2010), PG 1658+441 with $M \approx 1.31$ $M_\odot$ and $B \approx 2.3 \times 10^6$ G (Liebert et al., 1983; Schmidt et al., 1992), and PG 1031+234 with the highest magnetic field of $B \approx 10^9$ G (Külebi et al., 2009; Schmidt et al., 1986). The existence of very massive WDs has been revealed in several studies (Althaus et al., 2005, 2007; Camisassa et al., 2019; Castanheira et al., 2013; Curd et al., 2017; Gentile et al., 2018; Hermes et al., 2013; Jiménez-Esteban et al., 2018; Sousa et al., 2020a).

In addition, WDs rotate with periods of days or even years. Recently a pulsating WD named AR Scorpii has been discovered (see Marsh et al., 2016), which emits electromagnetic radiation ranging from X-rays to radio waves, pulsing in brightness with a period of 1.97 min. Furthermore, the X-ray emission has been proposed to be caused by a pulsar-like emission from a fast-spinning WD, suggesting that AR Sco is primarily a rotation-powered pulsar (RPP). Besides that, other sources have been proposed as candidates for WD pulsars. In particular, AE Aquarii, with a short spin period of $P = 33.08$ s (Terada et al., 2008). Furthermore, the X-ray Multimirror Mission XMM-Newton observatory has observed a WD rotating faster than AE Aquarii. It has been shown by Mereghetti et al. (2009) that the X-ray pulsator RX J0648.0-4418, which belongs to the binary systems HD 49798/RX J0648.0-4418, is a massive $M = 1.28$ $M_\odot$ white dwarf with a radius of around $R = 3000$ km and a very small spin period of $P = 13.2$ s. Also, Ashley et al. reported the discovery of strong pulsations with a period of 38.9 s in the *HST* ultraviolet data of V1460 (see Ashley et al., 2020). Very recently, Lopes et al. reported on XMM-*Newton* observations of CTCV J2056-3014 revealing that this object is an X-ray-faint intermediate polar harboring an extremely fast-spinning WD with a spin period of 29.6 s (see Lopes et a.l, 2020). Shortly thereafter, we used the equation of state (EoS) of a carbon WD accounting for electron-ion, electron-electron, and ion-ion interactions. For this EoS, we determined the mass density thresholds for the onset of pycnonuclear fusion reactions and investigated the impact of microscopic stability and of fast-rotation on the structure and stability of WDs. Our analysis has lead to a minimum mass for CTCV J2056-3014 of 0.56 $M_\odot$, and a maximum mass of around 1.38 $M_\odot$ (see Otoniel et al., 2020, for details).

It is worth mentioning that several models of highly magnetized and fast-spinning WDs have been proposed (see Mukhopadhyay et al., 2020;

4 *E. Otoniel, J.G. Coelho, M. Malheiro, and F. Weber*

Cáceres et al., 2016; Coelho and Malheiro, 2014; Gentile et al., 2018; Lobato et al., 2016; Malheiro et al., 2012; Sousa et al., 2020a,b; Vishal et al., 2014, and references therein). More recently, Kalita nd Mukhopadhyay (2019) show that continuous GWs can be emitted from rotating magnetized WDs and will possibly be detected by the upcoming gravitational wave (GW) detector (see also Sousa et al., 2020a,b). Furthermore, as pointed out in Sousa et al. (2020b), for the first time in the literature, it is estimated the GWs counterpart for Soft Gamma Repeaters (SGRs) and Anomalous X-Ray pulsars (AXPs) described as WD pulsars. They have found that some SGRs/AXPs can be observed by the space detectors BBO and DE-CIGO. In addition, the same authors have estimated the GW amplitude and luminosity for three binary systems that have a fast-spinning magnetized WD, namely, AE Aquarii, AR Scorpii and RX J0648.0-4418 (see Sousa et al., 2020a, for details).

Also, Rueda et al. (2013) have proposed a scenario that the optical/IR data are explained by the WD photosphere and by assuming the existence of an accretion disk (Rueda et al., 2013). Recently, a new scenario has been proposed to explain the spectral energy distribution of 4U0142+61, from mid-infrared up to hard X-rays (see Borges et al., 2020, and references therein). In this model the persistent emission comes from an accreting isolated massive and HMWD surrounded by a debris disk, having gas and dusty regions. This scenario is inspired by the periodic flux modulation and by the presence of mid-IR emission, which is rare for neutron stars (NSs) [appears only in about 0.3% of all isolated NSs]. On the other hand, the presence of mid-IR in WDs is quite common. Debes et al. (2011) found that about 7% of all isolated WDs exhibit an excess of mid-IR emission.

It has also been proposed by Subramanian and Mukhopadhyay (2015) that the light curves of some peculiar superluminous Ia supernovae could be explained by super-Chandrasekhar white dwarfs (SChWDs) whose masses are greater than the Chandrasekhar mass limit, $M_{Ch} = 1.44$ $M_\odot$. From a theoretical point of view, WDs can rotate at periods as short as $P \sim 0.5$ s (Boshkayev et al., 2013) and they can be formed in double WD mergers (Becerra et al., 2018; Garcia-Berro et al., 2012; Rueda et al., 2013). Livio and Pringle (1998) and Livio (1999) have investigated the role of rotation for the maximum mass of a uniformly rotating WD.

General relativistic effects on uniformly rotating white dwarfs have been studied more recently in (Boshkayev et al., 2013). In particular, fast-spinning WDs with extreme magnetic fields have been investigated in order to see how huge magnetic fields would change the mass and the radius of

these stars, affecting their spherical symmetry and stabilities (see, e.g., Angel, 1978; Bera and Bhattacharya, 2014, 2016; Das et al., 2014; Das and Mukhopadhyay, 2015; Franzon and Schramm, 2015). It has been shown by Franzon and Schramm (2015) that massive WDs can support magnetic fields at their center of up to $\sim 10^{15}$ G if they are non-rotating, and $\sim 10^{14}$ G if they are rapidly rotating. According to Das and Mukhopadhyay (2012), the effects of an extremely large and uniform magnetic field on the EoS of a WD could increase its critical mass up to 2.58 $M\odot$. This mass limit is reached for extremely large magnetic fields of $\sim 10^{18}$ G.

Also, a general relativistic magnetohydrodynamic (GRMHD) framework that describes rotating and magnetized axisymmetric WDs has been explored sequentially by Bera and Bhattacharya (2016); Subramanian and Mukhopadhyay (2015). Nevertheless, as already discussed in the literature (Chamel et al., 2014; Chamel and Fantina, 2015; Coelho et al., 2014), the breaking of spherical symmetry due to magnetic fields and microphysical effects, such as electron capture reactions and pycnonuclear reactions, can severely limit the magnetic fields inside WDs. In addition, calculations employing magneto-hydrodynamics (MHD) and a polytropic equation of state (EoS) with an adiabatic index $\Gamma = 4/3$ were performed in order to investigate the stability of SChWDs, considering poloidal and toroidal magnetic field configurations (see Das and Mukhopadhyay, 2015; Subramanian and Mukhopadhyay, 2015, and references therein). It was found that huge magnetic fields, up to 5×10^{15} G, may exist inside such high-mass WDs, and that their masses can be in the range of $2 - 3$ $M_\odot$. The internal magnetic fields can be much stronger than at the surface (see Franzon and Schramm, 2015; Otoniel et al., 2019, and references therein). Theoretical studies suggest that the magnetic field in the interior can be up to three orders of magnitude larger, i.e., $\sim 10^{12}$ G, than the largest observed surface magnetic fields, $\sim 10^8 - 10^9$ G (Franzon and Schramm, 2015). Recently, we have also shown that maximum-mass WDs could have masses of around 2.14 $M_\odot$ for a central magnetic field of $\sim 3.85 \times 10^{14}$ G, which indicates that highly magnetized white dwarfs may play a crucial role for the interpretation of superluminous type Ia supernovae. Furthermore, we note that pycnonuclear fusion reactions limit the central white dwarf density to $\lesssim 9.35 \times 10^9$ g/cm^3, which implies that the equatorial radii of white dwarfs cannot be much smaller than around 1100 km (see Otoniel et al., 2019). It is worth noting that general relativistic effects do not change the maximum mass of a WD but have a significant impact on the stellar radius (see, for instance, Carvalho et al., 2018).

6   *E. Otoniel, J.G. Coelho, M. Malheiro, and F. Weber*

Nuclear reactions have a determining role in the existence and evolution of several astrophysical environment (see Liccardo et al., 2018). These nuclear reactions have been found to occur over a significant range of stellar densities (Gasques et al., 2005), including the density range found in the interiors of WDs (Boshkayev et al., 2013). Recently, *static* WD calculations also showed that central energy densities are limited by nuclear fusion reactions and inverse β-decay (see Chamel et al., 2013, 2014; Chamel and Fantina, 2015). We have also investigated the properties of stationary and strongly magnetized WDs, taking into account the electron capture and pycnonuclear fusion reactions instabilities (Malheiro et al., 2021; Otoniel et al., 2019).

Here, we explore the properties of rotating WDs endowed with strong magnetic fields ($\sim 10^{12}$ G) using a modern EoS which accounts for electron-ion interactions among lattice nuclei, and which makes use of the latest experimental atomic mass data (Audi et al., 2012; Wang et al., 2012). We estimate the mass density thresholds for the onset of electron capture reactions and pycnonuclear reactions in the cores of massive and HMWDs, and explore the impact of microscopic stability and fast rotation on the structure and stability of different WD constitutions. We also note that the presence of ^{12}C $+^{16}$ O lattices in WDs reduces the Kepler periods (increases the Kepler frequencies) of WDs mildly, which has its origin in the softening of the EoS caused by the lattice. The softening leads to WDs with somewhat smaller radii and therefore smaller Kepler periods.

This chapter is organized as follows. In Sec. 2, we revisit the physics of an electron gas subjected to high magnetic fields. In Sec. 3, we introduce the model used for the EoS of HMWDs, which accounts for electron-ion interactions among lattice nuclei. In Sec. 4, we discuss the role of the electron capture and pycnonuclear fusion reactions for the structure and stability of HMWDs. In Sec. 5, we present the structure equations of WDs in hydrostatic equilibrium and present limits of the rotational frequencies of strongly magnetized WDs. The Kepler (mass shedding) frequency is used to set an absolute limit on stable stellar rotation. Features on non-spherical stars are discussed in Sec. 6. Finally, in Sec. 7 we present a summary of the main findings and concluding remarks.

2. Electron gas in strong magnetic fields

The increase of more sensitive techniques of observation and detection of WDs (Eisenstein et al., 2006), coupled with advanced calculations of the

properties of fermionic matter under extreme physical condition, has led to considerable interest in theoretical studies of the structure and evolution of white dwarfs (Chamel et al., 2014; Marsh et al., 2016; Mereghetti et al., 2009; Terada et al., 2008). Strong magnetic fields are known to modify the EoS used to describe the global structure of WDs (see, for instance, Coelho et al., 2014; Das and Mukhopadhyay, 2013, 2015; Otoniel et al., 2015, and references therein). Below we briefly summarize the equations which describe a relativistic electron gas (Canuto and Chiu, 1968; Potekhin and Chabrier, 2000, 2013; Potekhin and Yakovlev, 2012) in the presence of a constant magnetic field. The Lagrangian of such a system is given by (we work here with Gaussian units) (Canuto and Chiu, 1968)

$$\mathcal{L} = \mathcal{L}_e + \mathcal{L}_{int} + \mathcal{L}_\gamma \,, \tag{1}$$

where the first term on the right-hand-side describes free relativistic electrons, and is given by

$$\mathcal{L}_e = -\frac{1}{2}\hbar c(\bar{\psi}\gamma_\mu\partial_\mu\psi - \partial_\mu\bar{\psi}\gamma_\mu\psi) - m_e c^2\bar{\psi}\psi \,, \tag{2}$$

where c denotes the speed of light, m_e the electron mass, and $\hbar$ Planck's constant. The quantity ψ is the electron wave function, and $\bar{\psi} = \psi^\dagger\gamma_0$, where $\psi^\dagger$ is the Hermitian conjugate of ψ.

Interactions among the electrons are described by

$$\mathcal{L}_{int} = ie\bar{\psi}\gamma_\mu A_\mu\psi \,, \tag{3}$$

and photon contributions are taken into account through

$$\mathcal{L}_\gamma = -\frac{1}{2}\frac{\partial A_\mu}{\partial x_\nu}\frac{\partial A_\mu}{\partial x_\nu} \,, \tag{4}$$

where $\partial_\mu \equiv \frac{\partial}{\partial x_\mu}$ with Greek indices running from 1 to 4. The γ matrices are defined in Pauli-Dirac representation. The components of the four-vector potential $A_\mu = (i\phi, \mathbf{A})$ are the scalar electric potential ϕ and the three-vector potential $\mathbf{A}$, which is parallel to the z-axis, according to the gauge (Canuto and Chiu, 1968)

$$A_\mu(x) = \delta_{\mu 2}\, x_1\, \mathbf{B} \,, \tag{5}$$

where $\mathbf{B}$ denotes a constant external magnetic field.

To determine the EoS we consider the grand-canonical partition function,

$$Z = Tr\left[e^{-\beta(H_e - \mu_e N_e)}\right] \,, \tag{6}$$

where $\beta \equiv 1/k_B T$ with k_B the Boltzmann constant and T the temperature. The quantities H_e, μ_e, and N_e denote the Hamiltonian, chemical potential, and average number density of electrons, respectively. The latter is given by $N_e = \frac{1}{\beta} \frac{\partial \ln Z}{\partial \mu_e}$. The grand-canonical potential is given by

$$\Omega = -\frac{1}{\beta} \ln Z , \tag{7}$$

which leads for the electron gas to

$$
\begin{aligned}
\Omega_e = &- \sum_n g_n \frac{2eB}{\hbar c} \int_{-\infty}^{\infty} \frac{dp_z}{(2\pi)^2} \sqrt{p_z^2 c^2 + s_e(n)^2} \\
&- \frac{1}{\beta} \sum_n g_n \frac{2eB}{\hbar c} \int_{-\infty}^{\infty} \frac{dp_z}{(2\pi)^2} \\
&\times \left[\ln\left(1 e^{-\beta(E_e - \mu_e)}\right) + \ln\left(1 + e^{-\beta(E_e + \mu_e)}\right) \right].
\end{aligned} \tag{8}
$$

The quantity $g_n = 2 - \delta_{n0}$ describes the degeneracy of the Landau levels. For an occupied ground state, $n = 0$, one has $g_n = 1$. For $n \geq 1$ one has $g_n = 2$, which corresponds to doubly degenerate states. The quantity s_e is given by

$$s_e(n) = \sqrt{m_e^2 c^4 \left(1 + 2\frac{B}{B_c} n\right)}, \tag{9}$$

and the electron energies E_e are defined as

$$E_e = \sqrt{p_z^2 c^2 + m_e^2 c^4 \left(1 + 2\frac{B}{B_c} n\right)}, \tag{10}$$

where $B_c = \frac{m_e^2 c^3}{e\hbar} \approx 4.14 \times 10^{13}$ G is the so called critical magnetic field. The second integral on the right-hand-side of Eq. (8) is the finite-temperature contribution of electrons to Ω_e. For the limiting case of zero temperature, one obtains

$$\lim_{T \to 0} \frac{1}{\beta} \ln\left(1 + e^{-\beta(E_e - \mu_e)}\right) = (\mu_e - E_e)\theta(\mu_e - E_e), \tag{11}$$

$$\lim_{T \to 0} \frac{1}{\beta} \ln\left(1 + e^{-\beta(E_e + \mu_e)}\right) = 0. \tag{12}$$

The energy density of the system in the parallel and perpendicular directions to the magnetic field B in terms of the grand-canonical potential can be written as

$$\mathcal{E}_e = \Omega_e + \mu_e N_e + \frac{B^2}{8\pi}. \tag{13}$$

Therefore, it follows immediately that

$$
\begin{aligned}
\mathcal{E}_e = & \sum_{n=0}^{n_{\max}} \frac{eB}{(2\pi)^2 \hbar c} \left[\mu_e \sqrt{\mu_e^2 - s_e(n)^2} \right. \\
& \left. + s_e(n)^2 \ln \frac{\mu_e + \sqrt{\mu_e^2 - s_e(n)^2}}{s_e(n)} \right] + \frac{B^2}{8\pi} \, .
\end{aligned}
\tag{14}
$$

Similarly, the pressure parallel to the magnetic field follows from the grand-canonical potential as

$$
P_\parallel = -\Omega_e - \frac{B^2}{8\pi} \, ,
\tag{15}
$$

so that

$$
\begin{aligned}
P_\parallel = & \sum_{n=0}^{n_{\max}} g_n \frac{eB}{(2\pi)^2 \hbar c} \left[\mu_e \sqrt{\mu_e^2 - s_e(n)^2} \right. \\
& \left. - s_e(n)^2 \ln \frac{\mu_e + \sqrt{\mu_e^2 - s_e(n)^2}}{s_e(n)} \right] - \frac{B^2}{8\pi} \, .
\end{aligned}
\tag{16}
$$

The perpendicular pressure is given by

$$
P_\perp = -\Omega_e - B\mathcal{M}_e + \frac{B^2}{8\pi} \, ,
\tag{17}
$$

where $\mathcal{M}_e = -\left(\frac{\partial \Omega_e}{\partial B} \right)$ is the magnetization. This leads for the perpendicular pressure to

$$
\begin{aligned}
P_\perp = & \sum_{n=0}^{n_{\max}} g_n \frac{eB}{(2\pi)^2 \hbar c} \left[\mu_e \sqrt{\mu_e^2 - s_e(n)^2} - s_e(n)^2 \right. \\
& \times \left. \ln \frac{\mu_e + \sqrt{\mu_e^2 - s_e(n)^2}}{s_e(n)} \right] - \frac{em_e}{4\pi^2} \left(\sum_{n=0}^{n_{\max}} g_n \left[\mu_e \sqrt{\mu_e^2 - s_e(n)^2} \right. \right. \\
& - \left. \left. \left[s_e(n)^2 + 2s_e(n)\mathcal{C}_e \right] \ln \frac{\mu_e + \sqrt{\mu_e^2 - s_e(n)^2}}{s_e(n)} \right] \right) \\
& + \frac{B^2}{8\pi}
\end{aligned}
\tag{18}
$$

where $\mathcal{C}_e$ is given by $\mathcal{C}_e = \frac{B}{B_c} n m_e c^2 / \sqrt{2 \frac{B}{B_c} n + 1}$. It is possible to obtain a relationship between $P_\parallel$ and $P_\perp$ of the following form (see, e.g., Paret et al., 2015.a,.; Strickland and Dexheimer, 2012)

$$
P_\perp = P_\parallel - \mathcal{M}_e B \, .
\tag{19}
$$

10   *E. Otoniel, J.G. Coelho, M. Malheiro, and F. Weber*

In Fig. 1 we show the parallel and longitudinal pressures as a function of mass density for different magnetic field values. One sees that magnetic fields up to 10^{12} G have essentially no impact on the EoS. This begins to change for magnetic fields on the order of 10^{13} G, in which case the pressure becomes anisotropic, that is, the pressure in the direction parallel to B differs from the pressure in the orthogonal direction to B.
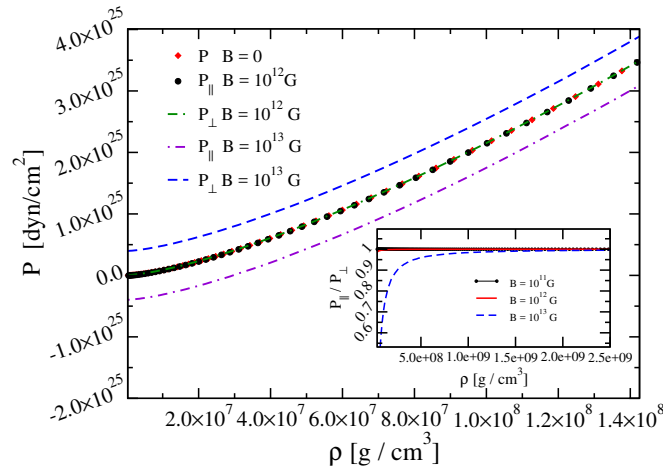

Fig. 1.   (Color online) Parallel and perpendicular pressures as a function of mass density, ρ. The orange diamond represents the $B = 0$ case. The inset shows $P_\parallel/P_\perp$ for magnetic fields ranging from 10^{11} to 10^{13} G.

3. Crystal Lattice

We assume that the core of a HMWD is composed of fully ionized ions forming a regular body-centered-cubic (bcc) crystal lattice (see Chamel et al., 2014, and references therein), referred to as regular crystal lattice (RCL) for short. Numerical simulations suggest that it is essential to take into account the effects of the Coulomb interaction in the EoS (Chamel and Haensel, 2008; Pearson et al., 2011), particularly when determining the maximum stable mass of a stationary WD (i.e., non-rotating) (Rotondo et al., 2011; Salpeter, 1961). This path has been followed for the investigations presented here. Originally, this model was used to describe the outer crust of a neutron star and later on to model the cores of super-dense WDs

Fast-spinning and highly magnetized white dwarfs   11

Table 1.   Lattice constants C, α, γ and parameters $(1-\alpha-\gamma)$ and ξ for a body-centered-cubic (bcc) crystal lattice structure of the model of Coldwell-Horsfall and Maradudin (see Chamel et al., 2014, for details).

Lattice	C	α	γ	$(1-\alpha-\gamma)$	ξ
bcc	-1.444231	0.389821	0.389821	0.220358	0.5

(Pearson et al., 2011).

The pressure at the center of a WD is essentially given by the pressure of degenerate electrons. However, due to the regular crystal lattice, the total pressure of WD matter is given by the sum of the degenerate electron and ionic lattice pressures,

$$P = P_e + P_L(Z, Z'),\tag{20}$$

where the pressure of the lattice, P_L, is given in terms of the energy density, $\mathcal{E}_L$, of the ionic lattice according to

$$P_L(Z, Z') = \frac{1}{3}\mathcal{E}_L,\tag{21}$$

with the lattice energy density given by (Chamel et al., 2014)

$$\mathcal{E}_L = Ce^2 n_e^{4/3} f(Z, Z').\tag{22}$$

The function $f(Z, Z')$ in Eq. (22) is given by

$$f(Z, Z') = \frac{\alpha Z^2 + \gamma Z'^2 + (1-\alpha-\gamma)ZZ'}{(\xi Z + (1-\xi)Z')^{4/3}},\tag{23}$$

with Z and Z' being the proton numbers of two different ions. The quantities C, α, γ are lattice constants. The values of the lattice constants together with ξ are listed in Table 1.

The total energy density is composed by the appropriate combination of degenerate electron gas, ions, ionic lattice, and the rest energy density of electrons as follows

$$\begin{aligned}\mathcal{E} = {}& n_x M(Z, A)c^2 + n_{x'} M(Z', A')c^2 + \mathcal{E}_e + \mathcal{E}_L \\ & - n_e m_e c^2.\end{aligned}\tag{24}$$

The quantities n_x and $n_{x'}$ are the number densities of nuclei with masses $M(Z, A)$ and $M(Z', A')$ (see, e.g., Audi et al., 2012; Wang et al., 2012, for the recent experimental nuclear masses of these nuclei).

E. Otoniel, J.G. Coelho, M. Malheiro, and F. Weber

4. Electron capture and pycnonuclear reactions in HMWDs

Highly magnetized white dwarfs with high central densities can became unstable to pycnonuclear and/or electron capture reactions (see Chamel et al., 2013, 2014; Chamel and Fantina, 2015; Coelho et al., 2014, and references therein). Electron capture by atomic nuclei, $A(N, Z) + e^- \to A(N + 1, Z - 1) + \nu_e$, leads to more neutron rich atomic nuclei in the cores of WDs. The loss of electrons in these reactions leads to an overall softening of the EoS of WD matter. The rate for this type of reaction is given by (Chamel et al., 2013)

$$\rho_\beta > \rho_\beta^{min} = \frac{B^\beta(A, Z)^{3/2}}{\sqrt{2}\pi^2\lambda^3}\frac{A}{Z}m\,, \tag{25}$$

where λ is the electron Compton wavelength, m is the neutron mass, and $B^\beta(A, Z)$ stands for the following relation,

$$B^\beta(A, Z) \equiv \frac{1}{2}\left(\frac{\mu_e^\beta(A, Z)}{m_e c^2}\right)^2\,. \tag{26}$$

The electron chemical potential is given by (Audi et al., 2012; Wang et al., 2012)

$$\mu_e \geq \mu_e^\beta(A, Z) \equiv \Delta(A, Z - 1) - \Delta(A, Z) + mc^2\,, \tag{27}$$

where $\Delta(A, Z)$ denotes the excess of nuclei mass, which for magnetic field strengths less than 10^{17} G is independent of the magnetic field (Pearson et al., 2011).

As discussed by Pearson et al. (2011) and Chamel et al. (2013), pycnonuclear fusion reactions might establish a more stringent limit on the microscopic stability of matter than electron capture reactions in ultramagnetized WDs (Gasques et al., 2005; Yakovlev et al., 2006). The rates of these reactions are however rather uncertain. The threshold density of pycnonuclear reactions is given by (Chamel et al., 2013; Pearson et al., 2011)

$$\rho_{\mathrm{pyc}} > \rho_{\mathrm{pyc}}^{min} = \frac{B^\beta(2A, 2Z)^{3/2}}{\sqrt{2}\pi^2\lambda^3}\frac{A}{Z}m\,. \tag{28}$$

Tables 2 and 3 show the threshold densities of inverse electron capture reactions and pycnonuclear fusion reactions in dense WD matter. Figure 2 illustrates the EoS of both dense non-magnetic as well as magnetic WD matter, with and without lattice contributions. The vertical lines show the densities at which pycnonuclear and electron capture (inverse-β) reactions set in (see the numerical values listed in Table 2 and 3). It is worth

Table 2.   Mass densities at which electron capture reactions in dense white dwarf matter made of a bcc crystal lattice set in. The values associated with $\rho_\beta^\star$ ignore contributions from electron-ion interactions. The densities listed in column ρ_β^0 are for zero magnetic fields, those in column $\rho_\beta^{\mathrm{BOSK}}$ are for the BOSK exponent of Boshkayev et al. (2013).

$_Z^A$X	ρ_β (g/cm^3)	$\rho_\beta^\star$ (g/cm^3)	ρ_β^0 (g/cm^3)	$\rho_\beta^{\mathrm{BOSK}}$ (g/cm^3)
$_2^4$He	1.32×10^{11}	1.28×10^{11}	1.72×10^{11}	1.39×10^{11}
$_6^{12}$C	3.12×10^{10}	2.93×10^{10}	3.94×10^{10}	3.97×10^{10}
$_8^{16}$O	1.55×10^{10}	1.43×10^{10}	1.92×10^{10}	1.94×10^{10}
$_{26}^{30}$Fe	1.05×10^{9}	8.76×10^{8}	1.18×10^{19}	1.18×10^{9}

Table 3.   Mass densities at which pycnonuclear reactions in dense white dwarf matter made of a bcc crystal lattice set in.   The threshold densities are computed from Eq. (28).   Electron-ion interactions have been neglected in the values listed for $\rho^\star$. The data shown in column ρ_{pyc}^0 are for zero magnetic field.

$_Z^A$X	ρ_{pyc} (g/cm^2)	$\rho_{\mathrm{pyc}}^\star$ (g/cm^2)	ρ_{pyc}^0 (g/cm^2)
$_2^4$He $+\,_2^4$He $\rightarrow\,_4^8$Be	5.17×10^{9}	4.93×10^{9}	6.63×10^{10}
$_6^{12}$C $+\,_6^{12}$C $\rightarrow\,_{12}^{24}$Mg	2.67×10^{9}	2.40×10^{9}	3.22×10^{9}
$_8^{16}$O $+\,_8^{16}$O $\rightarrow\,_{16}^{32}$S	1.37×10^{8}	1.20×10^{8}	1.61×10^{8}

mentioning that the threshold mass density above which matter becomes unstable against electron captures for different compositions are consistent with the results discussed by Chamel and Fantina (2015). In addition, the inclusion of the electron-ion interactions increases ρ_β, and the heavier the elements the larger the effect (see Chamel and Fantina, 2015). Lattice contributions soften the EoS, as can be seen in panel (B) of this figure. The EoS of magnetized matter is slightly softer than the EoS of non-magnetized matter.

5. Stellar structure equations

The structure of WDs is governed by hydrostatic equilibrium, where gravity is balanced by the outward pressure generated by a relativistic electron gas. Recently, it has been noted that contributions from general relativity (GR) ought to be taken into account when modeling the structure of white dwarfs (Boshkayev et al., 2013; Carvalho et. al, 2015; Rotondo et al., 2011). This is accomplished by making use of the Tolman-Oppenheimer-Volkoff (TOV) equations for the calculation of the properties of non-rotating WDs (Op-
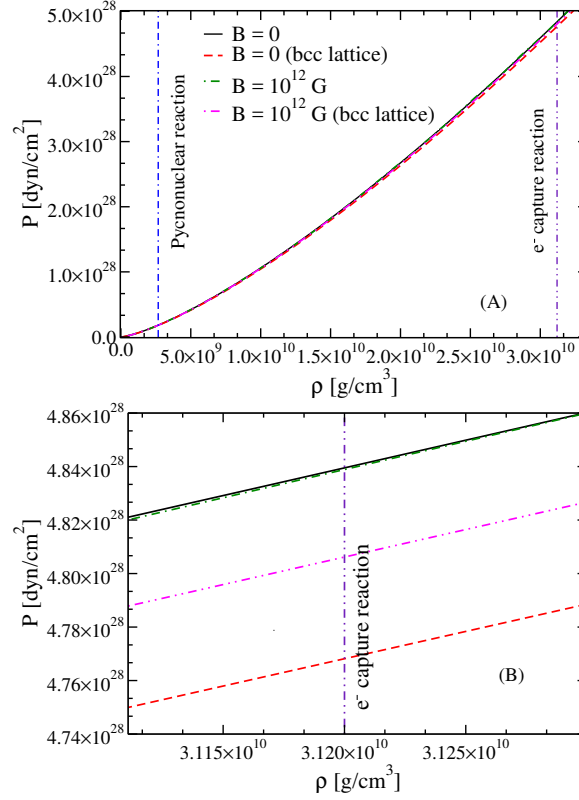
Fig. 2.   (Color online) Pressure-mass density relations for $B = 0$ and $B = 10^{12}$ G, with and without lattice contributions. An enlargement of the high-density part of panel (A) is shown in panel (B). The black (red) dashed lines are for $B = 0$ without (with) lattice contributions. The green dot-dashed (brown double dot-dashed) line are for $B = 10^{12}$ G without (with) lattice contributions. The vertical lines mark the onsets of pycnonuclear and electron capture (inverse-β) reactions.

penheimer and Volkoff, 1939; Tolman, 1939) . Adopting the geometric unit system $(G = c = 1)$, the TOV equation is given by

$$\frac{dP(r)}{dr} = -\frac{(\mathcal{E}(r) + P(r))(M(r) + 4\pi P(r)r^3)}{r^2(1 - 2M(r)/r)} \,, \tag{29}$$

where $M(r)$ denotes the gravitational mass contained inside a sphere of radius r. The amount of this mass is given by

$$\frac{dM(r)}{dr} = 4\pi\mathcal{E}(r)r^2 \,. \tag{30}$$

Fast-spinning and highly magnetized white dwarfs   15

As mentioned just above, the TOV equations describe the structure of non-rotating stellar objects. In order to account for rotational effects, Einstein's field equations need to be solved for a metric which accounts for rotational deformation and the dragging of local inertial frames (Friedman et al., 1986; Hartle and Thorne, 1967, 1968). Such a metric is given by (Friedman et al., 1986; Weber, 2005.a,.)

$$ds^2 = -e^{2\nu}dt^2 + e^{2\psi}(d\phi - \omega dt)^2 + e^{2\mu}d\theta^2 + e^{2\lambda}dr^2 \,, \tag{31}$$

where the metric functions ν, ψ, μ, λ and the frame dragging frequency, ω, depend on the radial coordinate r, the polar angle θ, and implicitly on the star's rotational frequency Ω (see Weber, 2005.b, for details). The latter is taken to be in the range of $0 \leq \Omega \leq \Omega_K$, with Ω_K denoting the Kepler (mass shedding) frequency. Ω_K sets an absolute upper limit on rapid rotation (Glendenning and Weber, 1994; Weber and Glendenning, 2012, 1991) and is given by (Friedman et al., 1986)

$$\Omega_{\rm K} = \omega + \frac{\omega'}{2\psi'} + e^{\nu-\psi}\sqrt{\frac{\nu'}{\psi'} + \left(\frac{\omega'}{2\psi'}e^{\psi-\nu}\right)^2} \,, \tag{32}$$

where the primes refer to partial derivatives with respect to the radial coordinate (Weber, 2005.b). The classical Newtonian limit of Eq. (32) is given by

$$\Omega_{\rm K} = \sqrt{M/R^3} \,, \tag{33}$$

where M denotes the star's gravitational mass and R its equatorial radius. The Kepler period, P_K, follows from $\Omega_{\rm K}$ as

$$P_{\rm K} \equiv \frac{2\pi}{\Omega_{\rm K}} \,. \tag{34}$$

The Kepler frequencies of carbon (^{12}C) white dwarfs with different magnetic fields and compositions are shown in Table 4. The masses and radii of the ^{12}C white dwarfs of this table are shown in columns 3 and 4 of Table 5. As can be seen, the general relativistic Kepler frequencies are smaller than the Newtonian frequencies, which is due to the existence of an axisymmetric instability region in the general relativistic case, which is absent in the Newtonian calculation (see Boshkayev et al., 2013). We also note that the bcc WDs shown in Table 4 have somewhat higher mass shedding frequencies than the WDs made of matter where ion-lattice contributions are ignored. This has its origin in the smaller equatorial radii of the bcc WDs caused by the attractive nature of the ion-lattice interactions.

16   *E. Otoniel, J.G. Coelho, M. Malheiro, and F. Weber*

Table 4.   Kepler frequencies of ^{12}C white dwarfs for different magnetic fields ($B = 0$ and $B = 10^{12}$ G), with and without body-centered-cubic (bcc) lattice contributions. The frequencies have been computed classically (Newton) from Eq. (33) as well as general relativistically (GR) from Eq. (32) using the formalism of Hartle and Thorne (Hartle and Thorne, 1967, 1968; Weber and Glendenning, 2012). The masses and radii of these stars are shown in Table 5.

Frequency	Method	$B = 0$ (no bcc lattice)	$B = 10^{12}$ G (bcc lattice)	$B = 10^{12}$ G (no bcc lattice)
$\Omega_{\mathrm{K}}^{\beta}$	GR	2.058 Hz	1.952 Hz	1.617 Hz
$\Omega_{\mathrm{K}}^{\beta}$	Newton	2.116 Hz	2.014 Hz	1.654 Hz
Ω_{K}^{GR}	GR	1.689 Hz	1.720 Hz	1.707 Hz
Ω_{K}^{GR}	Newton	1.742 Hz	1.776 Hz	1.762 Hz
$\Omega_{\mathrm{K}}^{\mathrm{pyc}}$	GR	0.727 Hz	0.698 Hz	0.667 Hz
$\Omega_{\mathrm{K}}^{\mathrm{pyc}}$	Newton	0.757 Hz	0.729 Hz	0.696 Hz

6. Spherical symmetry breaking

It was shown by Chandrasekhar and Fermi (1953) that the figure of equilibrium of an incompressible spherical fluid with an internal uniform magnetic field that matches an external dipole field is no longer represented by a sphere (see also Coelho et al., 2014, and references therein) but by an oblate spheroid instead. For a spherical fluid, the lowest-order surface correction can be expressed as (Chandrasekhar and Fermi, 1953)

$$r(\mu) = R + \epsilon P_l(\mu)\,, \tag{35}$$

where $P_l(\mu)$ is the Legendre polynomial of order l and $\mu = \cos\theta$ (θ denoting the polar angle). The quantity ϵ in Eq. (35) satisfies $\epsilon \ll R$ and measures the deviation from a spherical configuration. In lowest order, only terms up to second order in l contribute (Chandrasekhar and Fermi, 1953). The polar, R_{p}, and equatorial, R_{eq}, radii are then given by

$$R_{\mathrm{p}} = R + \epsilon P_l(1)\,, \tag{36}$$

$$R_{\mathrm{eq}} = R + \epsilon P_l(0)\,, \tag{37}$$

One can readily show that

$$\frac{\epsilon}{R} = \frac{R_{\mathrm{eq}} - R_{\mathrm{p}}}{R}\,, \tag{38}$$

for a non-spherical deformation with $l = 2$.

A magnetized star becomes unstable when a constant internal magnetic field deforms such a star to an oblate spheroid ($\epsilon < 0$) (see Coelho et al., 2014, for details). The stellar deformation proceeds until a limiting value for ϵ/R, given by

$$\frac{\epsilon}{R} = -\frac{15}{8}\frac{B^2 R^4}{GM^2}\,, \tag{39}$$

is reached. Using this condition, it is possible to determine which maximum magnetic field can be supported by a magnetized star, until the object becomes unstable due to the breaking of spherical symmetry. Using the expression for the gravitational potential energy, $-3GM^2/5R$, one has

$$\frac{1}{4}B_c^2 R^3 = -\frac{3}{5}\frac{GM^2}{R}\,, \tag{40}$$

and the deformation parameter given by Eq. (39) can be written as

$$\frac{\epsilon}{R} = -4.5\,B_\star^2\,, \tag{41}$$

where $B_\star = B/B_c$. It is worth mentioning that when the (constant) internal magnetic field of a magnetized star is close to the limiting value established by the virial theorem, the star tends to take on a highly oblate form, and thus becoming unstable (see Chandrasekhar and Fermi, 1953; Coelho et al., 2014, and references therein).

7. Discussion and Conclusions

The main objective of this chapter is to discuss lattice instabilities and the mass-radius relationship of HMWDs. Emphasis is also put on the role of stellar rotation on the properties of such objects.

Figure 3 shows the mass-radius relationships of HMWDs containing ^{12}C(50%)$+^{16}$O(50%) lattices in their interiors, for magnetic field strengths ranging from zero to 4.4×10^{13} G. As can be seen, magnetic fields increase both the mass and the radius of a WD, and the effects become more pronounced as the strength of B increases, which is consistent with the results shown by Ostriker and Hartwick (1968); Suh et al. (2000). It is also known from the literature that the radii of white dwarfs with a given gravitational mass increase with B. We confirm this feature for the EoS of our study. For a heavy WD, with a gravitational mass of around 1.2 M$_\odot$, for instance, we find that strong magnetic fields may lead to a radius increase of a few thousand kilometers, depending on the strength of the magnetic field. In the right panel of Figure 3, we show the deformation parameter, ϵ/R, of the magnetized white dwarf shown in the left panel of this figure. One sees that the deformation of the WDs increases (i.e., ϵ/R becomes more negative) with increasing B values. The fact that the deformation parameter is negative reveals that the WDs become more and more oblate if the magnetic field strength increases to larger values. This shows that spherical symmetry, and the concept of isotropic pressures in HMWDs, is no longer valid for large B values, a phenomenon also noted in Fig. 1.
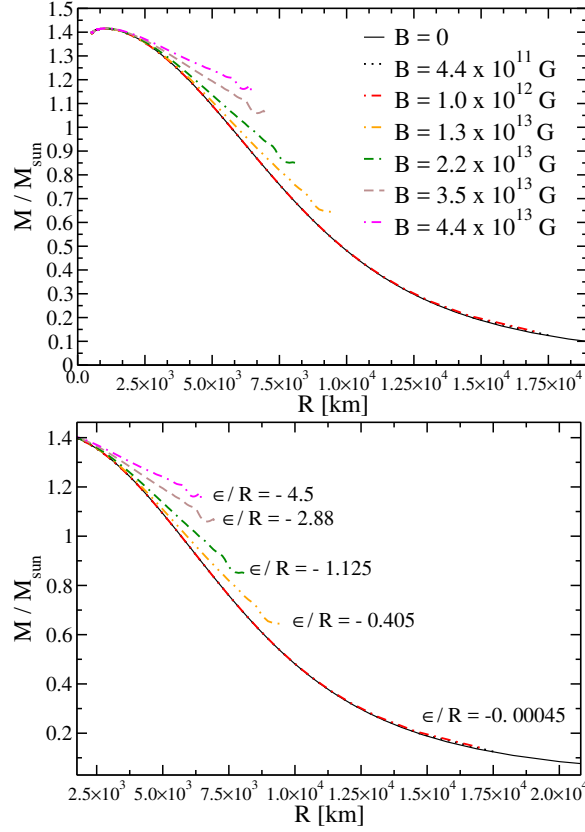
18   *E. Otoniel, J.G. Coelho, M. Malheiro, and F. Weber*

Fig. 3.   (Color online) Left panel: Mass-radius relationship of ^{12}C (50%) $+^{16}$O (50%) white dwarfs with magnetic fields up to 4.4×10^{13} G. Right panel: Radial stellar deformation parameter, ϵ/R (see text), of the white dwarfs shown in the left panel. The fact that $\epsilon/R < 0$ indicates that the stars possess oblate shapes.

Figure 4 shows the gravitational mass of non-rotating an well as rotating ^{12}C white dwarfs, as a function of central mass density. The latter rotate at the general relativistic Kepler frequency Ω_K, given by Eq. (32), at which mass shedding sets an absolute limit on rapid rotation. The masses of white dwarfs rotating at Ω_K are up to 0.15 M$_\odot$ more massive than non-rotating white dwarfs. The magnetic fields carried by the WDs of this figure is $B = 10^{12}$ G. Several additional important characteristic features are highlighted next. First, the light gray area shows the density at which

Fast-spinning and highly magnetized white dwarfs   19

pycnonuclear reactions are active inside of these WDs. These reactions set in at around 2×10^9 g/cm^3. The black square shows the location of the WD at the pycnonuclear reaction boundary. The mass (in units of M$_\odot$) and radius (in km) of this object are presented in parenthesis. Second, the narrow green area marks the density range over which an axisymmertric, general relativistic instability exists. Third, the yellow area shows the density regime for which the inverse-β reaction is present. The black circle and black triangle show the mass and radius values of white dwarfs located at the threshold densities at which these instabilities set in. Sumarizing, we find that the general relativistic instability sets in before inverse-β reaction occur in WD matter. The lowest threshold of all instabilities, however, is set by pycnonuclear fusion reactions. The rates of these reactions are however still rather uncertain (see Otoniel et al., 2019).
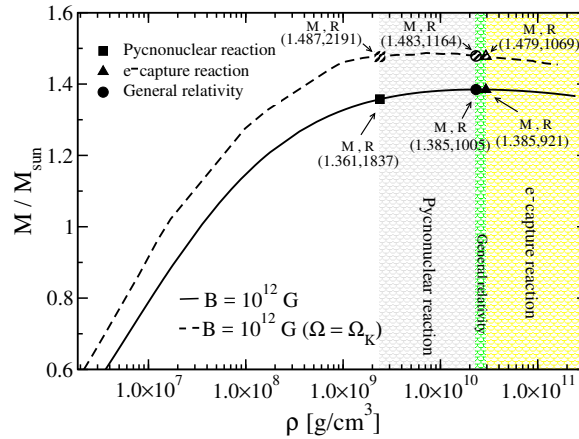

Fig. 4.   (Color online) Gravitational mass as a function of central mass density for a ^{12}C white dwarf with a magnetic field of $B = 1.0 \times 10^{12}$ G. The colored regions represent areas where WD matter is subject to pycnonuclear reactions, an axisymmetric general relativistic instability, and electron capture reactions.

Figure 5 shows the mass-radius relationships of non-rotating and rotating white dwarfs for a magnetic field of $B = 10^{12}$ G. The frequency of the rotating stars is the Keplers frequency given by Eq. (32). The EoS of these stars accounts for bcc lattice contributions. The dashed horizontal lines connect non-rotating and rotating WDs with the same baryon number ($\log_{10} A$) with each other. These lines represent potential evolutionary
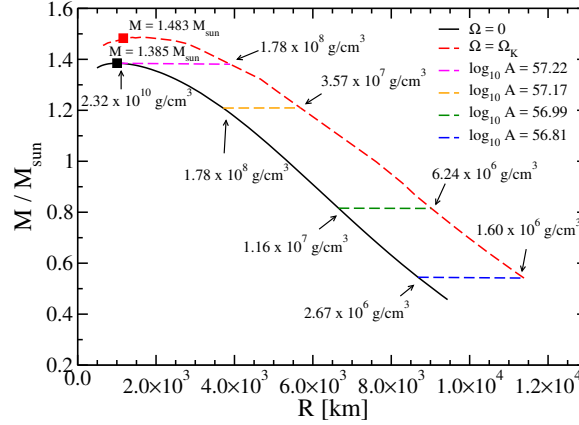
E. Otoniel, J.G. Coelho, M. Malheiro, and F. Weber

Fig. 5.   (Color online) Mass-radius relationships of non-rotating (sold black curve) and rotating (dashed red curve) bcc ^{12}C white dwarfs with a magnetic field of $B = 1.0 \times 10^{12}$ G. Several stellar paths are shown (dashed blue, green, orange and magenta lines) which isolated rotating WDs (fixed baryon numbers, $\log_{10} A$) would follow when spinning down from the Kepler frequency, $\Omega = \Omega_K$, to zero, $\Omega = 0$. The numerical values next to the arrows denote the mass densities in the cores of these stars.

tracks of isolated WDs spinning down from high to low frequencies, as the baryon numbers of such stars would remain unchanged. As can be read off from the figures associated with each evolutionary path, the change in the central mass densities of these WDs ranges from a factor ~ 2, for the lighter stars ~ 0.5 M$_\odot$ of the sequence, to ~ 100 for the most massive members of the sequence.

In Fig 6 we show the mass-radius relationships of non-rotating (black curve) and rotating (dashed red curve) ^{12}C (50%)+^{16}O (50%) white dwarfs carrying a magnetic field of $B = 10^{12}$ G. As already mentioned in connection with Fig. 5, the mass increase due to rotation at the Kepler frequency, Ω_K, is around 10%. We also note that the central densities of the rotating WDs are smaller than those of the non-rotating stars, since less pressure is to be provided by the EoS in the rotating case, and that the maximum-mass limit slightly decreases when lattice contributions are taken into account, which soften the EoS mildly (see Fig. 1).

Figure 7 shows the rotational deformation of a non-rotating ^{12}C $+^{16}$O white dwarf (with 1.384 M$_\odot$) caused by rotation at the Kepler frequency. The baryon number of both stars is the same, $\log_{10} A = 57.22$, but the their gravitational masses differ by a small amount because of rotation.
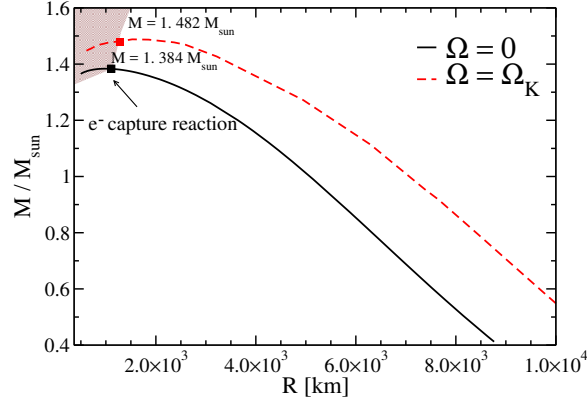
Fast-spinning and highly magnetized white dwarfs   21

Fig. 6.   (Color online) Mass-radius relationship of rotating and non-rotating magnetic $^{12}C + ^{16}O$ white dwarfs with bcc lattice contributions included. The colored area represents the regime where instabilities due to pycnonuclear reactions, electron-capture reactions, and general relativity are present.

The non-rotating WD has a mass of $M = 1.384$ M$_\odot$ and a corresponding central density of $\rho = 2.02 \times 10^{10}$ g/cm^3, while the mass of the rotating WD is $M = 1.376$ M$_\odot$ and $\rho = 2.14 \times 10^8$ g/cm^3. Hence this rotating white dwarf is around 94 times less dense than its non-rotating counterpart. The entire set of parameters of mass and radii taking into account different possibilities of instabilities to theses stars, constituted by ^{12}C and $^{12}C + ^{16}O$, is given in Table 5.

Figure 8 shows the Kepler period, $P_K = 2\pi/\Omega_K$ versus gravitational mass of selected magnetic white dwarf models with and without bcc lattice contributions. As can be seen, the presence of lattice contributions $^{12}C + ^{16}O$ WDs reduces the Kepler periods (increases the Kepler frequencies) of white dwarfs mildly, which has its origin in the softening of the EoS (see Fig. 2) caused by the lattice. The softening leads to white dwarfs with somewhat smaller radii and therefore smaller Kepler periods. Overall, one sees that very massive magnetic $^{12}C + ^{16}O$ white dwarfs have rotational Kepler periods on the order 0.5 s, which corresponds to a rotational frequency of 2.0 Hz. Pycnonuclear reactions are triggered in these WDs at masses that are markedly smaller than the maximum white dwarf masses. The corresponding rotational periods are turn out to be in the 5 second ($\sim$ 0.2 Hz) range.

A possible mechanism for the formation of SChWDs was proposed by

22   E. Otoniel, J.G. Coelho, M. Malheiro, and F. Weber

Table 5. Maximum gravitational masses of non-rotating ($\Omega = 0$) and rotating (at Kepler frequency, Ω_K) magnetic white dwarfs experiencing different interior physical processes (i.e., pycnonuclear (pyc) reactions, electron capture (inverse-β) reactions).

Quantity	Units	^{12}C $B = 10^{12}$ G (with bcc lattice)	^{12}C $B = 10^{12}$ G (without lattice)	^{12}C (50%) $+^{16}$O (50%) $B = 10^{12}$ G (with bcc lattice)	^{12}C (50%) $+^{16}$O (50%) $B = 10^{12}$ G (without lattice)
$M^\beta(\Omega = 0)$	M$_\odot$	1.385	1.412	1.384	1.415
$R_\mathrm{eq}(\Omega = 0)$	km	920.733	948.865	1131.792	1194.157
$M^\beta(\Omega = \Omega_\mathrm{K})$	M$_\odot$	1.484	1.501	1.479	1.486
$R_\mathrm{eq}(\Omega = \Omega_\mathrm{K})$	km	1069.151	1220.946	1306.720	1401.261
$M(\Omega = 0)$	M$_\odot$	1.385	1.412	1.482	1.509
$R_\mathrm{eq}(\Omega = 0)$	km	1004.845	1015.734	930.473	1034.863
$M(\Omega = \Omega_\mathrm{K})$	M$_\odot$	1.483	1.514	1.384	1.416
$R_\mathrm{eq}(\Omega = \Omega_\mathrm{K})$	km	1163.572	1277.795	1080.723	1270.691
$M^\mathrm{pyc}(\Omega = 0)$	M$_\odot$	1.361	1.389	1.478	1.495
$R_\mathrm{eq}(\Omega = 0)$	km	1836.84	1907.881	3782.966	4323.396
$M^\mathrm{pyc}(\Omega = \Omega_\mathrm{K})$	M$_\odot$	1.487	1.519	1.338	1.320
$R_\mathrm{eq}(\Omega = \Omega_\mathrm{K})$	km	2108.868	2190.988	4413.811	5319.416

Fast-spinning and highly magnetized white dwarfs 23
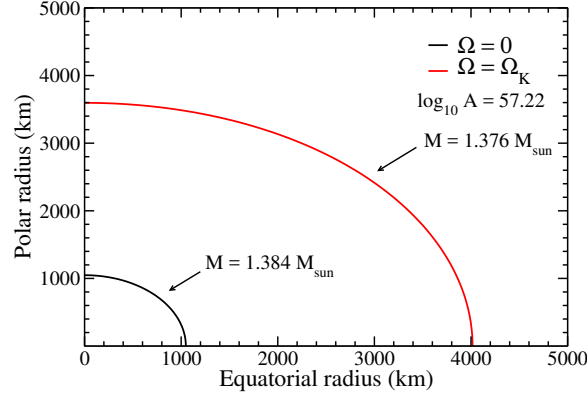

Fig. 7. (Color online) Radial profiles of two magnetized $^{12}C + ^{16}O$ white dwarfs with a same baryon number of $\log_{10} A = 57.22$. The end points of these curves show the polar and equatorial radii, R_{p} and R_{eq}, respectively. The red line is for a WD rotating at the Kepler frequency ($\Omega_{\mathrm{K}} = 1.952$ Hz), the black curve is for the same star but at zero rotation. The respective gravitational masses are $M = 1.376 M_\odot$ and $M = 1.384 M_\odot$.
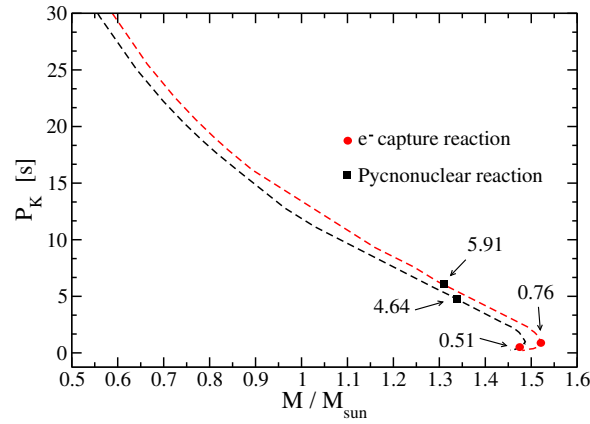

Fig. 8. (Color online) Kepler period, given by Eq. (34), versus mass of magnetic $^{12}C + ^{16}O$ white dwarfs ($B = 10^{12}$ G) with (black) and without (red) bcc lattice contributions. The numerical values next to the arrows display the rotational periods (in seconds) of a few selected WDs.

Das and Mukhopadhyay (2013) [and further extended in Das et al. (2013)], who suggested that such stars could be formed by mass accretion onto a

HMWD. As pointed out in (Coelho et al., 2014), electron capture reactions and pycnonuclear fusion reactions should play a significant role for the evolution of such a star from its low-mass configuration to its high-mass termination point. On the other hand, it is interesting to note that the most stringent limit on the magnetic fields of WDs is possibly set by type-Ia supernovae (Das and Mukhopadhyay, 2013). It the traditional picture, such an explosion is triggered when a white dwarf reaches its maximum-possible mass, the Chandrasekhar mass, but that no such explosion can occur before this mass is reached. In the traditional thermonuclear runaway model, however, a type-Ia supernova is triggered when the critical density $\rho_{\mathrm{ign}}^{\mathrm{C}}$ for carbon ignition inside of a white dwarf is reached. This value is not known precisely, but theoretical studies predict values for $\rho_{\mathrm{ign}}^{\mathrm{C}}$ in the range of 2–3×10^9 g/cm^3 (see, e.g. Lesaffre et al., 2006, and references therein). These $\rho_{\mathrm{ign}}^{\mathrm{C}}$ values are way lower than the critical densities at which instability against electron capture reactions and pycnonuclear reaction (discussed above) set in. Hence the latter may severely impact the evolution of white dwarfs as well.

An upper limit to the magnetic field can be obtained by equating the carbon ignition density $\rho_{\mathrm{ign}}^{\mathrm{C}}$ to the central stellar density of the magnetic field, $\rho_B = B_{\mathrm{center}}^2/8\pi c^2$. From this one obtains for the maximum magnetic field $B_{\mathrm{central}}^{\max} = c\sqrt{8\pi\rho_{\mathrm{ign}}^{\mathrm{C}}} \approx 6.7 \times 10^{15}$ G, which indicates that in order to prevent a premature type-Ia supernova explosion, lower magnetic fields need to exist at the center of a white dwarf in order to prevent a premature type-Ia supernova explosion.

Stellar rotation could be a possible explanation for super-Chandrasekhar WDs with central densities lower than $\rho_{\mathrm{ign}}^{\mathrm{C}}$ (Boshkayev et al., 2013). Besides, rotation could also be related to some superluminous type-Ia supernovae and supernova delay time distributions (see Ilkov and Soker, 2012, and references therein). However, this possibility does not seem to be plausible for the SChWDs model of Das and Mukhopadhyay (2013), since stellar configurations with large masses have densities up to three orders of magnitude larger than $\rho_{\mathrm{ign}}^{\mathrm{C}}$.

In summary, we have demonstrated here that the occurrence of pycnonuclear reactions and inverse beta reactions in the cores of highly magnetized WDs depends strongly on the rotation rate (and thus on the mass) of a WD. Rapid rotation increases the mass of a WD by up to 10%, accompanied by an up to hundredfold drop in central stellar density. Pycnonuclear reactions, for instance, are therefore triggered in rotation WDs at masses

that differ markedly from maximum WD masses. This study ought to lay the groundwork for future research on the multifaceted properties of fast, massive and highly magnetized WDs.

References

Althaus, L. G. and García-Berro, E. and Isern, J. and Córsico, A. H. (2005). *Mass-radius relations for massive white dwarf stars*, Astronomy & Astrophysics, **441**, pp.689-694.

Althaus, L. G. and García-Berro, E. and Isern, J. and Córsico, A. H. and Rohrmann, R. D. (2007). *The age and colors of massive white dwarf stars*, Astronomy & Astrophysics, **465**, pp.249-255.

Angel, J. R. P (1978). *Magnetic white dwarfs,*Annual Review of Astronomy and Astrophysics**16**, pp.487-519.

Ashley, R. P. and 8 colleagues (2020). *V1460 Her: a fast spinning white dwarf accreting from an evolved donor star.*Monthly Notices of the Royal Astronomical Society, **499**, pp. 149-160.

Audi, G. and Wang, Meng and Wapstra, A. H. and Kondev, F. G. and Mac-Cormick, M. and Xu, X. and Pfeiffer, B.*The Ame2012 atomic mass evaluation,*Chinese Physics C, **36**, pp.1287.

Banibrata and Sarkar, Arnab and Tout, Christopher A (2020). *Modified virial theorem for highly magnetized white dwarfs*, Monthly Notices of the Royal Astronomical Society, **500**, pp.763-771.

Barstow, M. A. and Jordan, S. and O'Donoghue, D. and Burleigh, M. R. and Napiwotzki, R. and Harrop-Allin, M. K.(1995). *RE J0317-853: the hottest known highly magnetic DA white dwarf*, Monthly Notices of the Royal Astronomical Society, **277**, pp.971-985.

Becerra, L. and Rueda, J. A. and Loren-Aguilar, P. and García-Berro, E. (2018). *The Spin Evolution of Fast-Rotating, Magnetized Super-Chandrasekhar White Dwarfs in the Aftermath of White Dwarf Mergers*, The Astrophysical Journal, **857**, pp.134.

Bera, Prasanta and Bhattacharya, Dipankar (2014). *Mass-radius relation of strongly magnetized white dwarfs: nearly independent of Landau quantization*, Monthly Notices of the Royal Astronomical Society,**445**, pp. 3951-3958.

26   *E. Otoniel, J.G. Coelho, M. Malheiro, and F. Weber*

Bera, Prasanta and Bhattacharya, Dipankar (2016). *Mass-radius relation of strongly magnetized white dwarfs: dependence on field geometry, GR effects and electrostatic corrections to the EOS, Monthly Notices of the Royal Astronomical Society*, **456**, pp. 3375-3385.

Boshkayev, Kuantay and Rueda, Jorge A. and Ruffini, Remo and Siutsou, Ivan (2013) *On general relativistic uniformly rotating white dwarfs, The Astrophysical Journal*, **762**, pp.117.

Boshkayev, Kuantay and Rueda, Jorge and Ruffini, Remo (2013) *On the maximum mass and minimum rotation period of relativistic uniformly rotating white dwarfs, International Journal of Modern Physics: Conference Series*, **23**, pp.193-197.

Cáceres, D. L. and de Carvalho, S. M. and Coelho, J. G. and de Lima, R. C. R. and Rueda, Jorge A. (2016). *Thermal X-ray emission from massive, fast rotating, highly magnetized white dwarfs, Monthly Notices of the Royal Astronomical Society*, **465**, pp.4434-4440.

Camisassa, María E. and Althaus, Leandro G. and Córsico, Alejandro H. and De Gerónimo, Francisco C. and Miller Bertolami, Marcelo M. and Novarino, María L. and Rohrmann, René D. and Wachlin, Felipe C. and García-Berro, Enrique (2019). *The evolution of ultra-massive white dwarfs, Astronomy & Astrophysics*, **625**, pp. A87.

Canuto, Vittorio and Chiu, Hong-Yee (1968). *Quantum Theory of an Electron Gas in Intense Magnetic Fields, Physical Review*, **173**, pp.1210-1219.

Carvalho, Geanderson and Jr, Rubens Marinho and Malheiro, Manuel (2015). *The importance of GR for the radius of massive white dwarfs, AIP Conference Proceedings*, **1693**, pp. 030004.

Carvalho, G. A. and Marinho, R. M. and Malheiro, M.(2018). *General relativistic effects in the structure of massive white dwarfs, General Relativity and Gravitation*, **50**, pp. 38.

Castanheira, B. G. and Kepler, S. O. and Kleinman, S. J. and Nitta, A. and Fraga, L. (2013). *Discovery of five new massive pulsating white dwarf stars, Monthly Notices of the Royal Astronomical Society*, **430**, pp. 50-59.

Chamel, N. and Fantina, A. F. and Davis, P. J. (2013) *Stability of super-Chandrasekhar magnetic white dwarfs, Physical Review D*, **88**, pp. 081301.

Chamel, N. and Molter, E. and Fantina, A.F. and Arteaga, D. P. (2014). *Maximum strength of the magnetic field in the core of the most massive white dwarfs, physical Review D*, **90**, pp. 043002.

Chamel, N. and Fantina, A. F. (2015). *Electron capture instability in magnetic and nonmagnetic white dwarfs, Chamel, N. and Fantina, A. F.,Physical review D*, **92**, pp. 023008.

Chamel, N. and Haensel, P. (2008). *Physics of Neutron Star Crusts, Living Reviews in Relativity*, **11**.

Chandrasekhar, S. and Fermi, E. (1953). *Problems of Gravitational Stability in the Presence of a Magnetic Field., The Astrophysical Journal*, **118**, pp.116.

Coelho, J. G. and Marinho, R. M. and Malheiro, M. and Negreiros, R. and Cáceres, D. L. and Rueda, J. A. and Ruffini, R. (2014). *Dynamical Instability of White Dwarfs and Breaking of Spherical Symmetry Under the*

Presence of Extreme Magnetic Fields, The Astrophysical Journal, **794**, pp. 86.

Coelho, J. G. and Malheiro, M. (2014). *Magnetic Dipole Moment of SGRs and AXPs Described as Massive and Magnetic White Dwarfs*, Publications of the Astronomical Society of Japan, **66**, pp. 14.

Curd, Brandon and Gianninas, A. and Bell, Keaton J. and Kilic, Mukremin and Romero, A. D. and Allende Prieto, Carlos and Winget, D. E. and Winget, K. I. (2017). *Four new massive pulsating white dwarfs including an ultramassive DAV*, Monthly Notices of the Royal Astronomical Society, **468**, pp. 239-249.

Das, Upasana and Mukhopadhyay, Banibrata and Rao, A. R. (2013). *A possible evolutionary scenario of highly magnetized super-chandrasekhar white dwarfs: progenitors of peculiar type ia supernovae*, The Astrophysical Journal, **767**, pp. L14.

Das, Upasana and Mukhopadhyay, Banibrata (2014). *Maximum mass of stable magnetized highly super-Chandrasekhar white dwarfs: stable solutions with varying magnetic fields*, Journal of Cosmology and Astroparticle Physics, **2014**, pp. 050.

Das, Upasana and Mukhopadhyay, Banibrata (2012) *Strongly magnetized cold degenerate electron gas: Mass-radius relation of the magnetized white dwarf*, Physical Review D, **86**.

Das, Upasana and Mukhopadhyay, Banibrata (2013). *New Mass Limit for White Dwarfs: Super-Chandrasekhar Type Ia Supernova as a New Standard Candle*, Physical Review Letters, **110**, pp. 071102.

Das, Upasana and Mukhopadhyay, Banibrata (2015). *GRMHD formulation of highly super-Chandrasekhar magnetized white dwarfs: stable configurations of non-spherical white dwarfs*, Journal of Cosmology and Astroparticle Physics, **2015**, pp. 016.

Debes, J. H. and Hoard, D. W. and Wachter, S. and Leisawitz, D. T. and Cohen, M. (2011). *The WIRED Survey. II. Infrared Excesses in the SDSS DR7 White Dwarf Catalog*, apjs, **197**, pp. 38.

Eisenstein, D. J. and Liebert, J. and Harris, H. C. and Kleinman, S. J. and Nitta, A. and Silvestri, N. and Anderson, S. A. and Barentine, J. C. and Brewington, H. J. and Brinkmann, J. and Harvanek, M. and Krzesiski, J. and Neilsen, Jr., Eric H. and Long, D. and Schneider, D. P. and Snedden, S. A. (2016). *A Catalog of Spectroscopically Confirmed White Dwarfs from the Sloan Digital Sky Survey Data Release 4*, The Astrophysical Journal Supplement Series, **167**, pp. 40-58.

Ferrario, L. and de Martino, D. and Gaensicke, B. T. (2015). *Magnetic White Dwarfs*, Space Science Reviews, **191**, pp. 111-169.

Franzon, B. and Schramm (2015). *Effects of magnetic fields and rotation on white dwarf structure*, Physical Review D, **92**.

Friedman, J. L. and Ipser, J. R. and Parker, L. (1986) *Rapidly rotating neutron star models*, The Astrophysical Journal, **304**, pp. 115-139.

García-Berro, Enrique and Lorén-Aguilar, Pablo and Aznar-Siguán, Gabriela and Torres, Santiago and Camacho, Judit and Althaus, Leandro G. and Córsico,

28   *E. Otoniel, J.G. Coelho, M. Malheiro, and F. Weber*

Alejandro H. and Kúlebi, Baybars and Isern, Jordi (2012). *Double degenerate mergers as progenitors of high-field magnetic white dwarfs*, *The Astrophysical Journal*, **749**, pp. 25.

Gasques, L. R. and Afanasjev, A. V. and Aguilera, E. F. and Beard, M. and Chamon, L. C. and Ring, P. and Wiescher, M. and Yakovlev, D. G. (2005) *Nuclear fusion in dense matter: Reaction rate and carbon burning*, *Physical Review C*, **72**.

Gentile Fusillo, N. P. and Tremblay, Pier-Emmanuel and Gänsicke, B. T and Manser, C. J and Cunningham, T. and Cukanovaite, E. and Hollands, M. and Marsh, T. and Raddi, R. and Jordan, S. and Toonen, S. and Geier, S. and Barstow, M. and Cummings, J. D. (2018).*A Gaia Data Release 2 catalogue of white dwarfs and a comparison with SDSS*, *Monthly Notices of the Royal Astronomical Society*, **482**, pp. 4570-4591.

Glendenning, N. K. and Weber, F. (1994). *Impact of frame dragging on the Kepler frequency of relativistic stars*, *Physical Review D*, **50**, pp. 3836-3841.

Hartle, James B. and Thorne, Kip S. (1967) *Slowly Rotating Relativistic Stars. I. Equations of Structure*, *The Astrophysical Journal*, **150**, pp. 1005.

Hartle, James B. and Thorne, Kip S. (1968). *Slowly Rotating Relativistic Stars. II. Models for Neutron Stars and Supermassive Stars*, *The Astrophysical Journal*, **153**, pp. 807.

Hermes, J. J. and Kepler, S. O. and Castanheira, Barbara G. and Gianninas, A. and Winget, D. E. and Montgomery, M. H. and Brown, Warren R. and Harrold, Samuel T.(2013). *Discovery of an Ultramassive Pulsating White Dwarf*, *Astrophysical Journal Letters*, **771**, pp. L2.

Ilkov, Marjan and Soker, Noam (2012). *Type Ia supernovae from very long delayed explosion of core-white dwarf merger: SNe Ia from core-white dwarf merger*, *Monthly Notices of the Royal Astronomical Society*, **419**, pp. 1695-1700.

Jiménez-Esteban, F. M. and Torres, S. and Rebassa-Mansergas, A. and Skorobogatov, G. and Solano, E. and Cantero, C. and Rodrigo, C. (2018). *A white dwarf catalogue from Gaia-DR2 and the Virtual Observatory*, *Monthly Notices of the Royal Astronomical Society*, **480**, pp. 4505-4518.

Kalita, Surajit and Mukhopadhyay, Banibrata (2019). *Continuous gravitational wave from magnetized white dwarfs and neutron stars: possible missions for LISA, DECIGO, BBO, ET detectors*,*Monthly Notices of the Royal Astronomical Society*, **490**, pp. 2692-2705.

Kepler, S. O. and Kleinman, S. J. and Pelisoli, I. and Peçanha, V. and Diaz, M. and Koester, D. and Castanheira, B. G. and Nitta, A. (2010). *Magnetic White Dwarfs in the SDSS and Estimating the Mean Mass of Normal DA and DB WDs*, *American Institute of Physics Conference Series*, **1273**,pp. 19-24.

Kepler, S. O. and Pelisoli, I. and Jordan, S. and Kleinman, S. J. and Koester, D. and Külebi, B. and Peçanha, V. and Castanheira, B. G. and Nitta, A. and Costa, J. E. S. and Winget, D. E. and Kanaan, A. and Fraga, L. (2013). *Magnetic white dwarf stars in the Sloan Digital Sky Survey*, *Monthly Notices of the Royal Astronomical Society*, **429**, pp. 2934-2944.

Kepler, S. O. and Pelisoli, I. and Koester, D. and Ourique, G. and Kleinman,

Fast-spinning and highly magnetized white dwarfs 29

S. J. and Romero, A. D. and Nitta, A. and Eisenstein, D. J. and Costa, J. E. S. and Külebi, B. and Jordan, S. and Dufour, P. and Giommi, P. and Rebassa-Mansergas, A. (2015).*New white dwarf stars in the Sloan Digital Sky Survey Data Release 10*, Monthly Notices of the Royal Astronomical Society,pp. 4078-4087.

Külebi, B. and Jordan, S. and Euchner, F. and Gänsicke, B. T. and Hirsch, H. (2009).*Analysis of hydrogen-rich magnetic white dwarfs detected in the Sloan Digital Sky Survey, Astronomy and Astrophysics*, **506**, pp. 1341-1350.

Külebi, B. and Jordan, S. and Euchner, F. and Gaensicke, B. T. and Hirsch, H. (2010).*Magnetic fields in white dwarfs (Kuelebi+, 2009), VizieR Online Data Catalog*, **350**, pp. 61341.

Külebi, B. and Jordan, S. and Nelan, E. and Bastian, U. and Altmann, M.(2010).*Constraints on the origin of the massive, hot, and rapidly rotating magnetic white dwarf RE J 0317-853 from an HST parallax measurement, Astronomy and Astrophysics*, **524**, pp. A36.

Lesaffre, P. and Han, Z. and Tout, C. A. and Podsiadlowski, P. and Martin, R. G. (2006). *The C flash and the ignition conditions of Type Ia supernovae, Monthly Notices of the Royal Astronomical Society*, **368**,pp. 187-195.

Liccardo, V. and Malheiro, M. and Hussein, M. S. and Carlson, B. V. and Frederico, T. (2018).*Nuclear processes in astrophysics: Recent progress, European Physical Journal A*, pp. 221.

Liebert, J. and Schmidt, G. D. and Green, R. F. and Stockman, H. S. and McGraw, J. T. (1983). *Two hot, low-field magnetic DA white dwarfs, The Astrophysical Journal*, **264**, pp. 262-272.

Livio, Mario (1999).*The Spins of White Dwarfs and Pulsars,***157**, *Annapolis Workshop on Magnetic Cataclysmic Variables*, pp. 247.

Livio, Mario and Pringle, J. E. (1998). *The Rotation Rates of White Dwarfs and Pulsars, The Astrophysical Journal*, **505**, pp. 339-343.

Lobato, Ronaldo V. and Malheiro, Manuel and Coelho, Jaziel G. (2016), *Magnetars and white dwarf pulsars, International Journal of Modern Physics D*, **25**, pp. 1641025.

Lopes de Oliveira, R. and Bruch, A. and Rodrigues, C. V. and Oliveira, A. S. and Mukai, K. (2020). *CTCV J2056-3014: An X-Ray-faint Intermediate Polar Harboring an Extremely Fast-spinning White Dwarf, Astrophysical Jornal Letters*, **898**,pp. L40.

Malheiro, M., Otoniel, E., Coelho, J. G. (2021). *Relevance of Dynamical Nuclear Processes in Quantum Complex Systems of Massive White Dwarfs ,Brazilian Journal of Physics*, **51**, pp. 223-230.

Malheiro, M. and Rueda, J. A and Ruffini, R. (2012). *SGRs and AXPs as Rotation-Powered Massive White Dwarfs, Publications of the Astronomical Society of Japan*, **64**, pp. 56.

Marsh, T. R. and Gänsicke, B. T. and Hümmerich, S. and Hambsch, F.-J. and Bernhard, K. and Lloyd, C. and Breedt, E. and Stanway, E. R. and Steeghs, D. T. and Parsons, S. G. and Toloza, O. and Schreiber, M. R. and Jonker, P. G. and van Roestel, J. and Kupfer, T. and Pala, A. F. and Dhillon, V. S. and Hardy, L. K. and Littlefair, S. P. and Aungwerojwit, A. and

30   *E. Otoniel, J.G. Coelho, M. Malheiro, and F. Weber*

Arjyotha, S. and Koester, D. and Bochinski, J. J. and Haswell, C. A. and Frank, P. and Wheatley, P. J.(2016). *A radio-pulsing white dwarf binary star*, Nature,**537**, pp. 374-377.

Mereghetti, S. and Tiengo, A. and Esposito, P. and La Palombara, N. and Israel, G. L. and Stella, L. (2009). *An Ultramassive, Fast-Spinning White Dwarf in a Peculiar Binary System*, Science, **325**, pp. 1222.

Oppenheimer, J. R. and Volkoff, G. M. (1939). *On Massive Neutron Cores*, Physical Review, **55**, pp. 374-381.

Ostriker, Jeremiah P. and Hartwick, F. D. A. (1969). *Rapidly Rotating Stars.IV. Magnetic White Dwarfs*, The Astrophysical Journal, **153**, pp. 797.

Otoniel, E., Coelho, J. G., Malheiro, M., Weber, F. (2020). *Mass limits of the extremely fast-spinning white dwarf CTCV J2056-3014*, arXiv e-prints.

Otoniel, E. and Franzon, B. and Carvalho, G. A. and Malheiro, M. and Schramm, S. and Weber, F. (2019). *Strongly Magnetized White Dwarfs and Their Instability Due to Nuclear Processes*, The Astrophysical Journal, **879**, pp. 46.

Otoniel, E and Malheiro, M and Coelho, J G (2015). *Fermionic matter under the effects of high magnetic fields and its consequences in white dwarfs*, Journal of Physics: Conference Series, **630**, pp. 012039.

Paret, Daryel Manreza and Horvath, Jorge Ernesto and Martínez, Aurora Pérez (2015). *Anisotropic stellar structure equations for magnetized strange stars*, Research in Astronomy and Astrophysics, **15**, pp. 975-985.

Paret, Daryel Manreza and Horvath, Jorge Ernesto and Martínez, Aurora Pérez (2015). *Maximum mass of magnetic white dwarfs*, Research in Astronomy and Astrophysics, **15**, pp. 1735-1741.

Pearson, J. M. and Goriely, S. and Chamel, N. (2011). *Properties of the outer crust of neutron stars from Hartree-Fock-Bogoliubov mass models*, Physical Review C, **83**.

Potekhin, Alexander Y. and Chabrier, Gilles (2000). *Equation of state of fully ionized electron-ion plasmas. II. Extension to relativistic densities and to the solid phase*, Physical Review E, **62**, pp. 8554-8563.

Potekhin, A. Y. and Chabrier, G. (2013). *Equation of state for magnetized Coulomb plasmas*, Astronomy & Astrophysics, **550**, pp. A43.

Potekhin, A. Y. and Yakovlev, D. G. (2012). *Comment on "Equation of state of dense and magnetized fermion system"*, Physical Review C, **85**, pp. 039801.

Rotondo, Michael and Rueda, Jorge A. and Ruffini, Remo and Xue, She-Sheng (2011). *Relativistic Feynman-Metropolis-Teller theory for white dwarfs in general relativity*, Physical Review D, **84**.

Rueda, J. A. and Boshkayev, K. and Izzo, L. and Ruffini, R. and Lorén-Aguilar, P. and Külebi, B. and Aznar-Siguán, G. and García-Berro, E. (2013). *A White Dwarf Merger as Progenitor of the Anomalous X-Ray Pulsar 4U 0142+61?*, The Astrophysical Journall, **772**, pp. L24.

Salpeter, E. E. (1961). *Energy and pressure of a zero-temperature plasma.*, The Astrophysical Journal, **134**, pp. 669.

Sarah V. Borges and Claudia V. Rodrigues and Jaziel G. Coelho and Manuel Malheiro and Manuel Castro (2020). *A magnetic white dwarf accretion model*

for the anomalous X-ray pulsar 4U 0142+61, The Astrophysical Journal, **895**, pp. 26.

Schmidt, G. D. and Bergeron, P. and Liebert, J. and Saffer, R. A.(1992). *Two ultramassive white dwarfs found among candidates for magnetic fields, Astrophysical Journal,* **394**, pp. 603.

Schmidt, G. D. and West, S. C. and Liebert, J. and Green, R. F. and Stockman, H. S.(1986). *The new magnetic white dwarf PG 1031 + 234 - Polarization and field structure at more than 500 milion Gauss, The Astrophysical Journal,* **309**, pp. 218.

Strickland, M. and Dexheimer, V. and Menezes, D. P. (2012). *Bulk properties of a Fermi gas in a magnetic field, Physical Review D,* **86**, pp. 125032.

Sousa, Manoel F. and Coelho, Jaziel G. and de Araujo, José C. N. (2020a). *Gravitational waves from fast-spinning white dwarfs, Monthly Notices of the Royal Astronomical Society,* **492**, pp. 5949.

Sousa, Manoel F and Coelho, Jaziel G and de Araujo, José C N (2020b). *Gravitational waves from SGRs and AXPs as fast-spinning white dwarfs, Monthly Notices of the Royal Astronomical Society,* **498**, pp. 4426.

Subramanian, S. and Mukhopadhyay, B. (2015). *GRMHD formulation of highly super-Chandrasekhar rotating magnetized white dwarfs: stable configurations of non-spherical white dwarfs, Monthly Notices of the Royal Astronomical Society,* **454**, pp. 752.

Suh, InSaeng and Mathews, G. J. (2000). *Mass-radius relation for magnetic white dwarfs, The Astrophysical Journal,* **530**, pp. 949.

Terada, Y. and Hayashi, T. and Ishida, M. and Mukai, K. and Dotani, T. and Okada, S. and Nakamura, R. and Naik, S. and Bamba, A. and Makishima, K. (2008). *Suzaku discovery of hard X-Ray pulsations from a rotating magnetized white dwarf, AEAquarii, Publications of the Astronomical Society of Japan,* **60**, pp. 387.

Tolman, Richard C. (1939). *Static solutions of Einstein's field equations for spheres of fluid, Physical Review,* **55**, pp. 364

Vishal, M. V. and Mukhopadhyay, Banibrata (2014). *Revised density of magnetized nuclear matter at the neutron drip line, Phys. Rev. C,* **89**, pp. 065804.

Wang, M. and Audi, G. and Wapstra, A. H. and Kondev, F. G. and MacCormick, M. and Xu, X. and Pfeiffer, B. (2012). *The Ame2012 atomic mass evaluation, Chinese Physics C,* **36**, pp. 1603.

Weber, F. (2005). *Strange quark matter and compact stars, Progress in Particle and Nuclear Physics,* **54**, pp. 193.

Weber, Fridolin (2005). *Pulsars as Astrophysical Laboratories for Nuclear and Particle Physics, Bristol, Philadelphia, USA.*

Weber, F. and Glendenning, N. K. (2012). *Application of the improved Hartle method for the construction of general relativistic rotating neutron star models, The Astrophysical Journal,* **390**, pp. 541.

Weber, F. and Glendenning, N. K. and Weigel, M. K. (1991). *Structure and stability of rotating relativistic neutron stars, The Astrophysical Journal,* **373**, pp. 579.

Yakovlev, D. G. and Gasques, L. R. and Afanasjev, A. V. and Beard, M. and Wi-

E. Otoniel, J.G. Coelho, M. Malheiro, and F. Weber

escher, M.(2006). *Fusion reactions in multicomponent dense matter*, *Physical Review C*, **74**, pp. 035803.